Electronic supplementary information

Morphochemical Imprinting of Melamine Cyanurate Mesocrystals into Glucose-derived Carbon for High Performance Lithium Ion Batteries

Jae Ho Kim,[‡a] Minhoo Byeon,[‡a] Yo Chan Jeong,[a] Jun Young Oh,[ab] Yeonsu Jung,[a]

Nina Fechler,[c] Seung Jae Yang[*b] and Chong Rae Park[*a]

[a.] Carbon Nanomaterials Design Laboratory, Research Institute of Advanced Materials, Department of Materials Science and Engineering, Seoul National University, Seoul 151-744, Republic of Korea, *E-mail: crpark@snu.ac.kr

[b.] Department of Applied Organic Materials Engineering, Inha University, Incheon 402-751, Republic of Korea, *E-mail: sjyang@inha.ac.kr

[c.] Department of Colloid Chemistry, Max Planck Institute of Colloids and Interfaces, MPI Campus Golm, Am Mühlenberg 1, 14476 Potsdam, Germany

‡ These authors contributed equally.

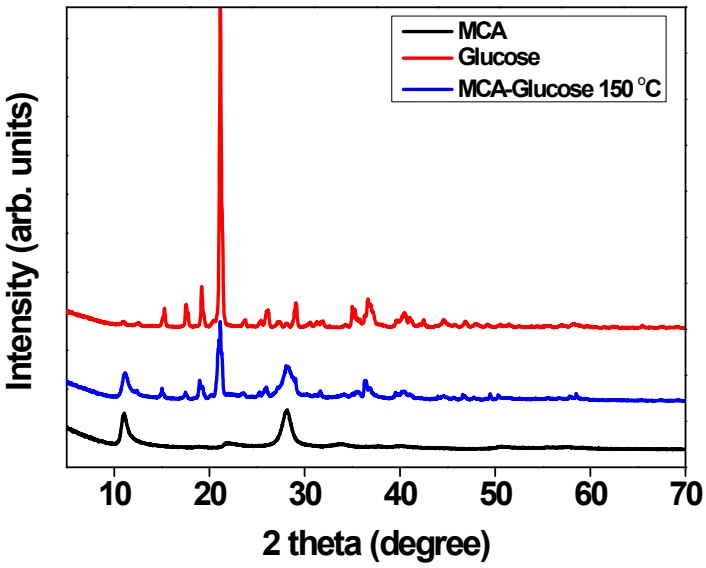

Fig. S1. XRD pattern of the MCA, glucose, and MCA with glucose after 150 ˚C heat treatment.

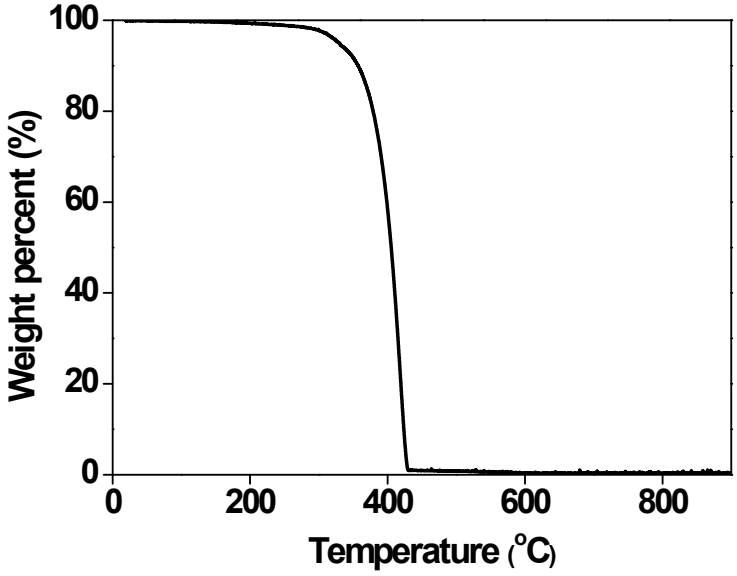

Fig. S2. Thermogravimetric analysis of the MCA under a nitrogen flow at a heating rate of 10 ˚C/min.

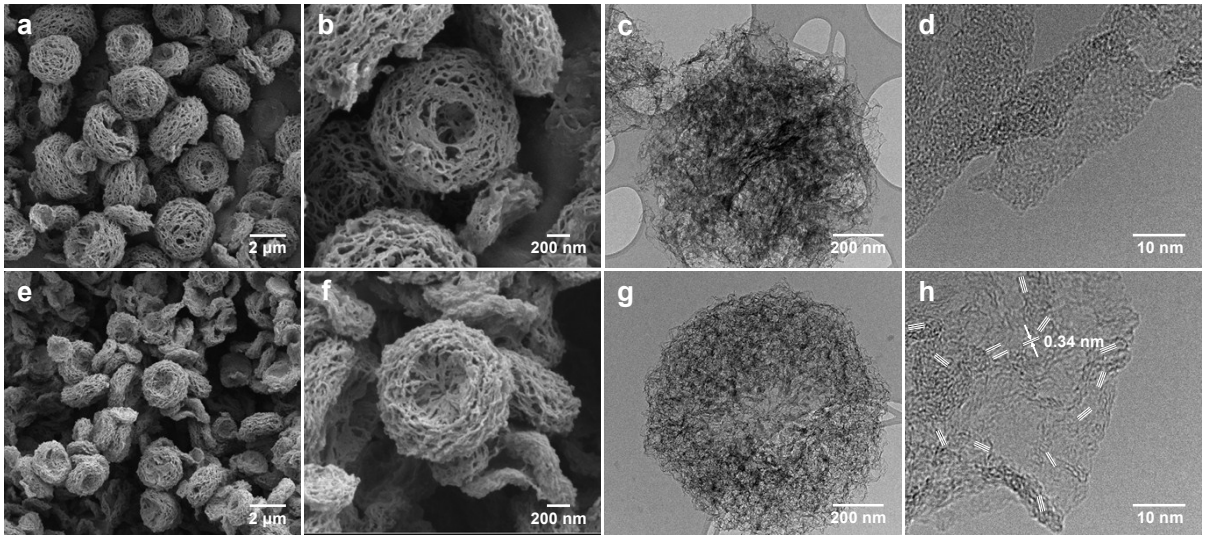

Fig. S3. SEM and TEM images of the NC7 (a-d) and NC9 (e-h).

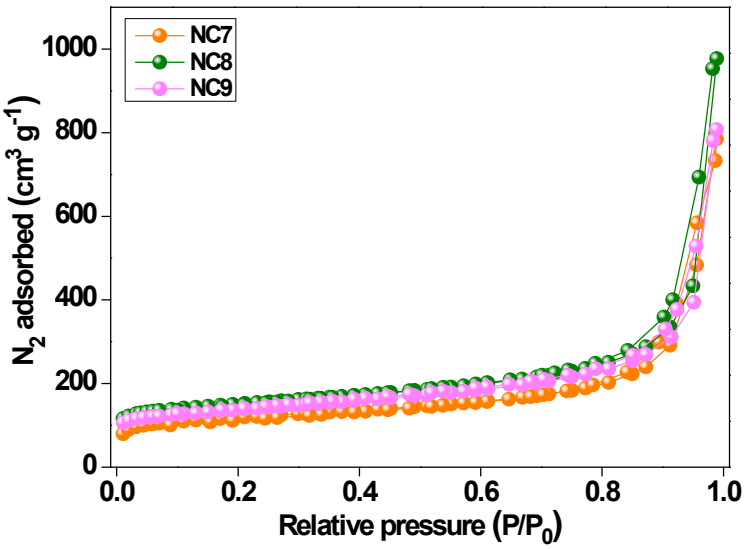

Fig. S4. N_2 isotherms at 77 K of the NC samples.

Table S1. Summary of pore characteristics and nitrogen bonding state of the NC samples.

Samples	N_2 isotherms		XPS				EA
	S_{BET} (m^2 g^{-1})	V_p (cm^3 g^{-1})	N (at%)	Pyridinic N (%)	Pyrrolic N (%)	Graphitic N (%)	N (at%)
NC7	433.7	1.21	25.5	48.2	25.6	26.1	24.4
NC8	559.5	1.51	19.9	44.5	20.0	35.5	19.7
NC9	496.1	1.25	11.4	38.7	17.0	44.3	10.6

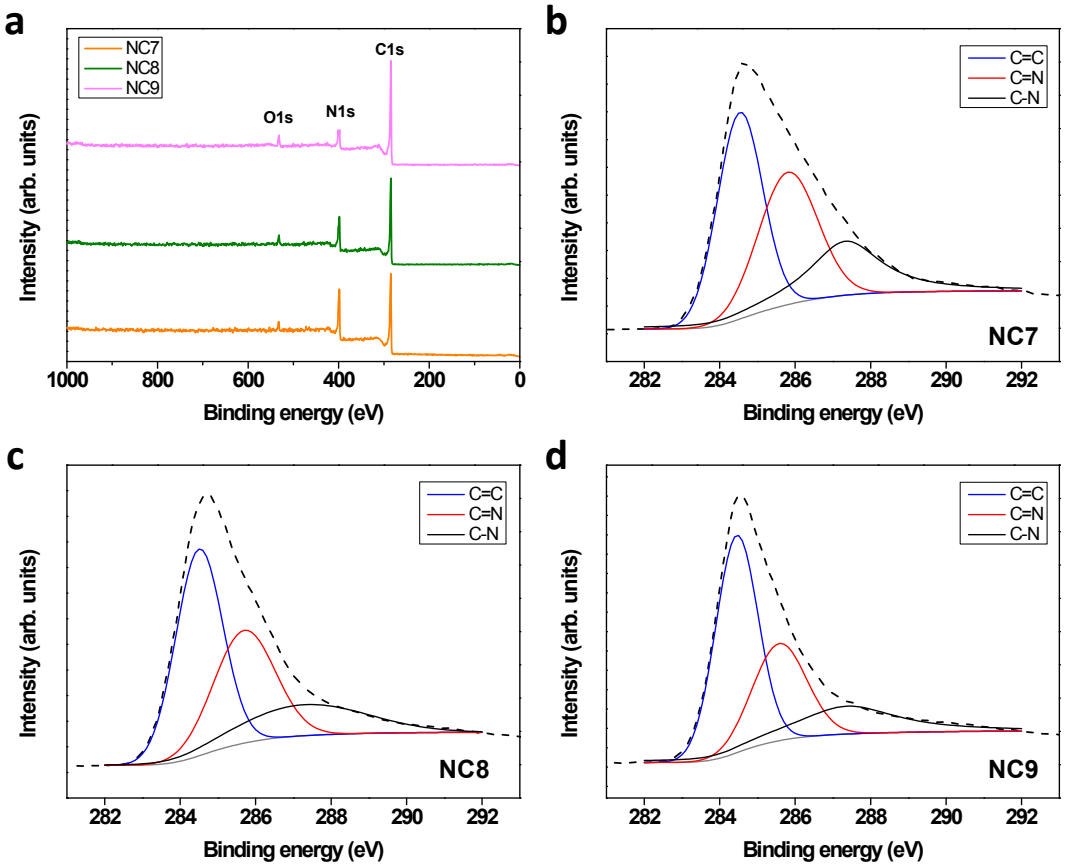

Fig. S5. a) XPS wide spectrum of the NC samples and high-resolution C1s spectra of the NC7 b), NC8 c), and NC9 d).

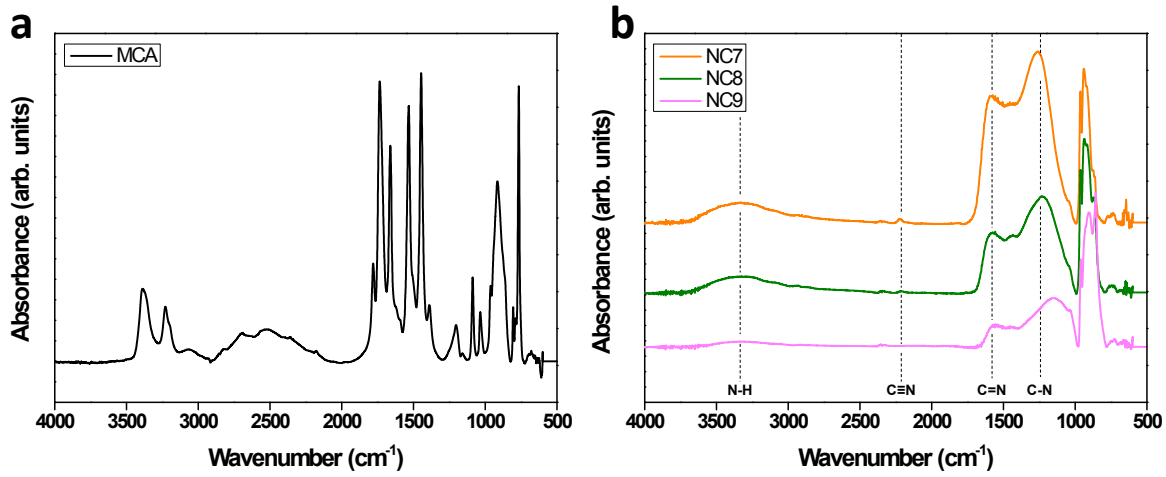

Fig. S6. IR spectra of the MCA a) and NC samples b).

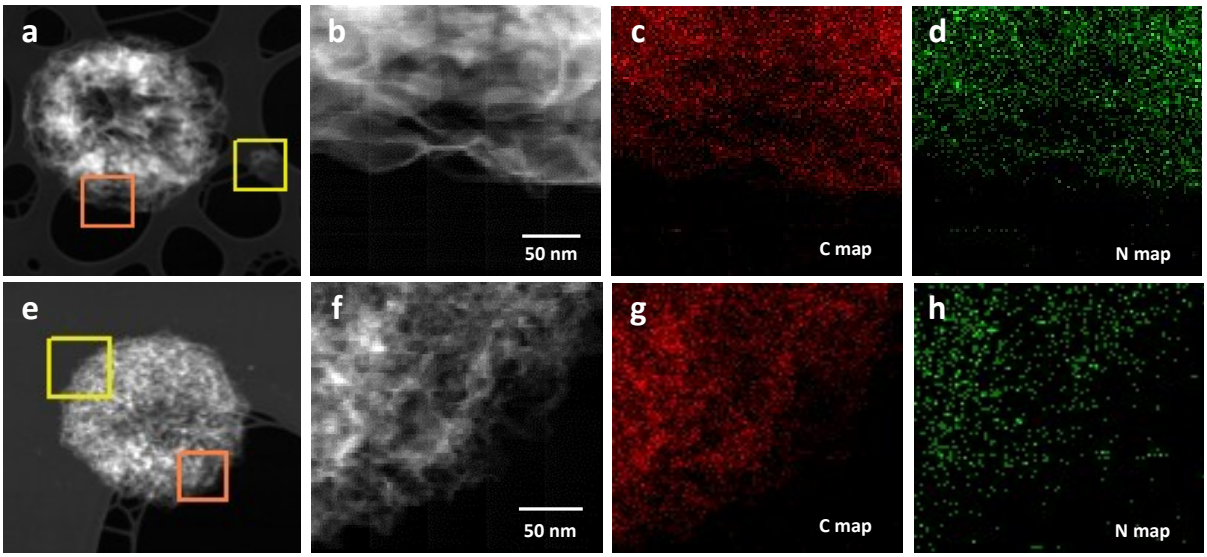

Fig. S7. TEM and STEM images of the NC7 (a-d) and NC9 (e-h) followed by elemental maps of carbon (red) and nitrogen (green).

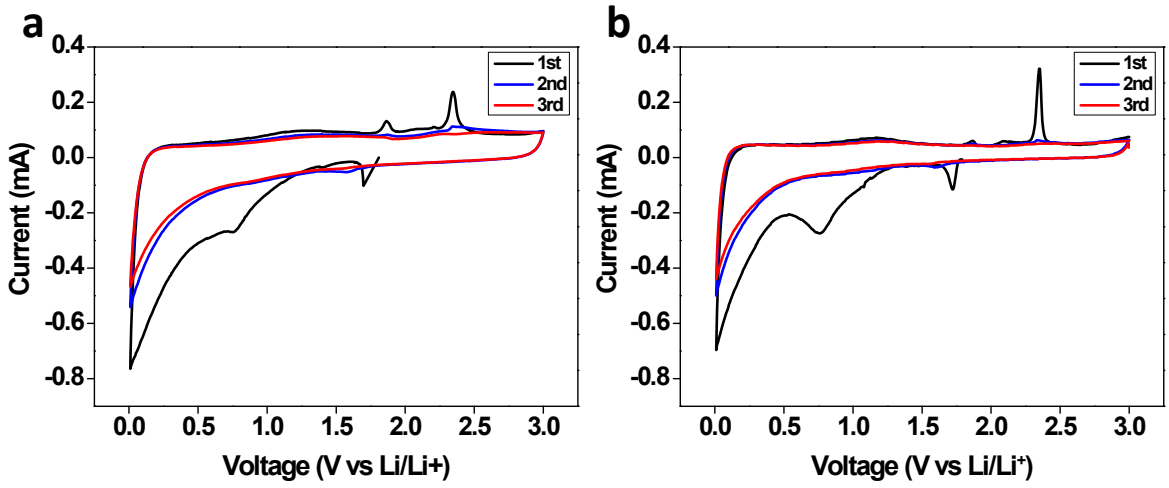

Fig. S8. CV curves of the NC7 (a) and NC9 (b) electrode at a sweep rate of 0.1 mV s-1 during the first three cycles.

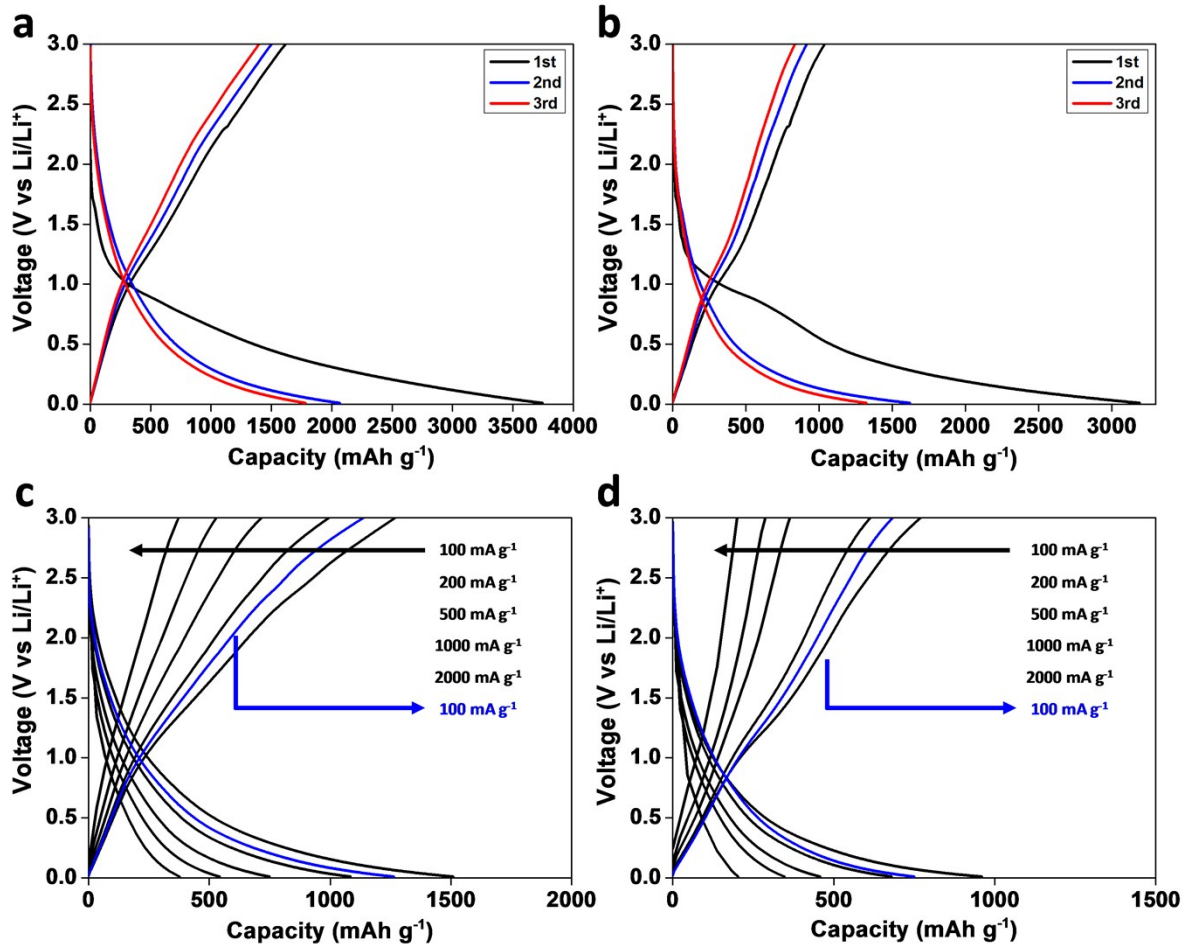

Fig. S9. Charge/discharge voltage profiles for the first three cycles of the NC7 (a) and NC9 electrodes at 100 mA g-1. The charge/discharge voltage profiles at different current densities of the NC7 (c) and NC9 (d) electrodes.

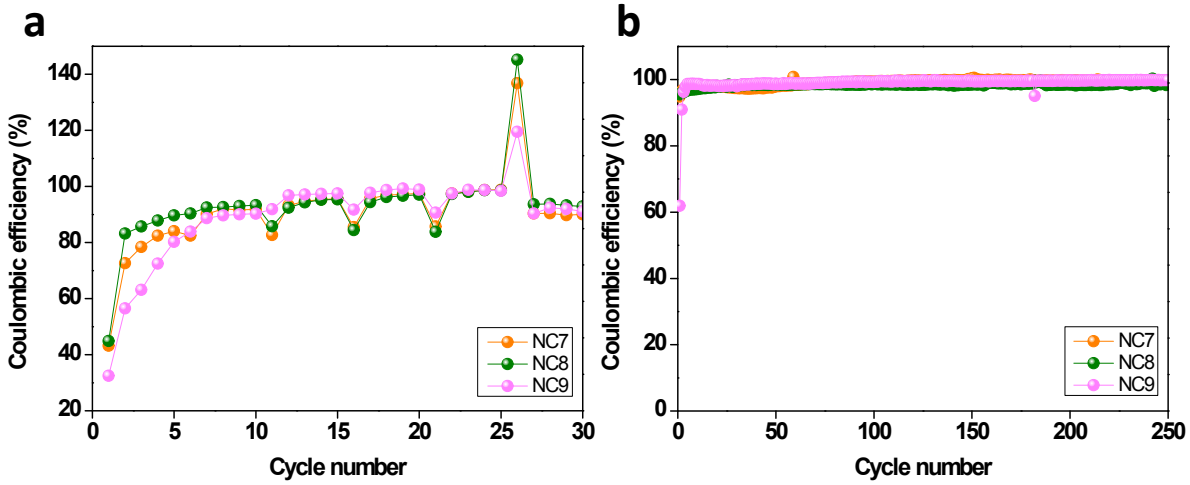

Fig. S10. Coulombic efficiency of the NC7, NC8, and NC9 electrode for (a) the rate capability test (corresponding to Fig. 4d) and (b) long-term cycle test (corresponding to Fig. 4e).

Table S2. Summary of the EIS results of the NC electrodes and graphite anode

Samples	R_s (Ω)	R_{ct} (Ω)	σ_w ($\Omega\ s^{-1/2}$)	D_{Li} ($cm^2\ s^{-1}$)
NC7	3.1	30.3	33.1	2.54×10^{-11}
NC8	3.8	23.7	4.4	1.43×10^{-9}
NC9	3.5	41.7	11.9	1.95×10^{-10}
Graphite	3.2	21.3	106.5	2.45×10^{-12}